Published in final edited form as:
Genesis. 2014 August ; 52(8): 752–758. doi:10.1002/dvg.22788.

Generation of a *Magoh* conditional allele in mice

John J. McMahon[1], **Lei Shi**[1], and **Debra L. Silver**[1,2,3]

[1]Department of Molecular Genetics and Microbiology, Duke University Medical Center, Durham, NC 27710

[2]Department of Cell Biology, Duke University Medical Center, Durham, NC 27710

[3]Department of Neurobiology and Duke Institute for Brain Sciences, Duke University Medical Center, Durham, NC 27710

Abstract

Magoh encodes a core component of the exon junction complex (EJC), which binds mRNA and regulates mRNA metabolism. *Magoh* is highly expressed in proliferative tissues during development. EJC components have been implicated in several developmental disorders including TAR syndrome, Richieri-Costa-Pereira Syndrome, and intellectual disability. Existing germline null *Magoh* mice are embryonic lethal as homozygotes and perinatal lethal as heterozygotes, precluding detailed analysis of embryonic and postnatal functions. Here we report the generation of a new genetic tool to dissect temporal and tissue specific roles for *Magoh* in development and adult homeostasis. This *Magoh* conditional allele has two LoxP sites flanking the second exon. Ubiquitous Cre-mediated deletion of the floxed allele in a heterozygous mouse ($Magoh^{del/+}$) causes 50% reduction of both *Magoh* mRNA and protein. $Magoh^{del/+}$ mice exhibit both microcephaly and hypopigmentation, thus phenocopying germline haploinsufficient *Magoh* mice. Using *Emx1-Cre,* we further show that conditional *Magoh* deletion in neural progenitors during embryonic development also causes microcephaly. We anticipate this novel conditional allele will be a valuable tool for assessing tissue specific roles for *Magoh* in mammalian development and postnatal processes.

Keywords

Conditional allele; microcephaly; Magoh; exon junction complex; cre; lox

Magoh is a core component of the exon junction complex (EJC), which also consists of Rbm8a, Eif4a3, and Casc3 (Zhao et al. 2000). The EJC binds spliced mRNA and influences mRNA metabolism in the nucleus and cytoplasm, including splicing of long-intron containing transcripts, mRNA localization, protein translation and nonsense-mediated decay (Kataoka et al. 2001; Le Hir et al. 2001; Nott, Le Hir, and Moore 2004; Palacios et al. 2004; Bono and Gehring 2011; Roignant and Treisman 2010; Ashton-Beaucage et al. 2010). Mouse and human MAGOH are highly conserved, showing 100% identity at the protein level. *Magoh* is highly expressed in many proliferative populations throughout development,

Corresponding author: debra.silver@duke.edu, (phone) 919-668-7909, (fax) 919-684-2790.

including the brain where it has been shown to play a critical role (Silver et al. 2010; Silver et al. 2013). Moreover it continues to be expressed in postnatal tissues (Allen Brain Atlas) (Singh et al. 2013). Thus, Magoh is predicted to be important for development of many organs, and for homeostatic function in adults.

In humans, EJC components have recently been implicated in several developmental diseases. *RBM8A* falls within a small micro-deletion/duplication on 1q21.1 associated with intellectual disability and altered brain size (Sharp et al. 2006). Individuals carrying compound mutations for this deletion and a regulatory mutation of *RBM8A* present with the blood and bone disorder, TAR syndrome (Albers et al. 2012). Mutations in *EIF4A3* cause Richieri-Costa-Pereira syndrome, a craniofacial disorder associated with both limb and neurological deficits (Favaro et al. 2014). Moreover, copy number changes in either *RBM8A* or *EIF4A3* are seen in patients exhibiting intellectual disability and brain malformations (Nguyen et al. 2013). Mutations of another EJC component, *UPF3B*, are associated with X-linked intellectual disability, schizophrenia and autism (Tarpey et al. 2007; Addington et al. 2011). These studies collectively indicate that EJC components are critical for pathogenesis of various developmental diseases. Yet we have a very limited understanding of how EJC components function in normal mammalian development.

Our group recently generated an ENU mutation in mice resulting in a germline null *Magoh* allele (termed $Magoh^{Mos2/+}$) (Silver et al. 2010; Matera et al. 2008). Heterozygous $Magoh^{Mos2/+}$ mice demonstrate a 50% reduction in *Magoh* mRNA and protein. Using this mouse model we discovered *Magoh* regulates development of the brain and pigment cells (Silver et al. 2010; Silver et al. 2013). However the $Magoh^{Mos2/+}$ allele is limited in its utility. First, it does not enable tissue specific deletion or cell autonomous functions of *Magoh*. Second, $Magoh^{Mos2/Mos2}$ mice are early embryonic lethal prior to E9.5, thus homozygous loss-of-function at later stages is unknown (Silver et al. 2010). Third, $Magoh^{Mos2/+}$ mice are perinatal lethal, prohibiting analysis of postnatal functions. Here we describe the generation of a new conditional allele of *Magoh*, which will enable the investigation of *Magoh* function in a temporal, spatial, and dosage specific manner during development and in adult homeostasis.

To establish a conditional *Magoh* knockout mouse we utilized gene targeting followed by FLP and Cre mediated recombinase excision (Fig. 1a). We obtained a targeting “knockout-first” vector, with *loxP* sites flanking exon 2, from the KOMP consortium. The targeting construct included a neomycin resistance selection cassette and a LacZ gene with a splice acceptor site, both flanked by FRT sites. The targeting vector was electroporated into C57BL/6J embryonic stem cells. Positive targeted clones were detected by southern blotting using probes against the 5′ and 3′ arms (Figs. 1a,b, Supplementary Fig. 1). Positive clones were confirmed using long-range PCR with primers against 5′ and 3′ arms (Figs 1a,c) (14/194 positive clones detected by both methods). Four positive ES clones were injected into Balb/c blastocysts, and subsequently implanted into pseudopregnant mice. Chimeric progeny (high percentage of black coat color) derived from one of these clones was selected for breeding and subsequent expansion of the line. Progeny were crossed to FLP-deleter mice to excise the neomycin resistance cassette and LacZ insertion, thus creating the conditional mouse ($Magoh^{lox/lox}$). $Magoh^{lox/lox}$ mice were viable and fertile with no overt

phenotype. We confirmed germline transmission of the floxed *Magoh* allele by genotyping with 2 sets of genomic primers designed against the first intron, the second intron, and the intron1-exon2 junction (Fig. 1d).

To assess functional deletion of *Magoh* we bred $Magoh^{lox/lox}$ mice with a ubiquitous germline Cre driver, *Ddx4-Cre. Ddx4-Cre;* $Magoh^{lox/+}$ males were then crossed with C57BL/6J females, producing $Magoh^{del/+}$ mice. We confirmed excision of exon 2 in these mice by genotyping (Fig. 1d). The resulting excision of exon 2 is predicted to generate a null *Magoh* allele, due to a frameshift resulting in a premature stop codon and subsequent nonsense-mediated decay (NMD) of the mutant transcript. We assessed Magoh protein levels by western blot of E12.5 cortical lysates collected from control and $Magoh^{del/+}$ brains. We observed a single band of Magoh at 17 KDa, but no bands at 11 KDa, where a truncated protein would be predicted to migrate (Fig. 2a). Relative to control, $Magoh^{del/+}$ cortices showed a ∼50% reduction in Magoh protein levels (Figs. 2a, b). This indicates the $Magoh^{del/+}$ transcript likely underwent NMD, as predicted. This finding was corroborated by qRT-PCR, which revealed a 50% reduction of *Magoh* mRNA in E12.5 cortices relative to control (Fig. 2c). Together this establishes that *Ddx4-Cre* mediated deletion of $Magoh^{lox/+}$ abolishes Magoh expression, similar to the existing germline $Magoh^{Mos2/+}$ allele.

We next assessed the functional impact of conditional deletion of *Magoh* by evaluating two phenotypes present in $Magoh^{Mos2/+}$ mice. We previously showed that *Magoh* germline haploinsufficient mice exhibit microcephaly due to defective embryonic neurogenesis (Silver et al. 2010). *Emx1-Cre* drives expression in the embryonic developing brain, specifically in neural progenitors of the dorsal telencephalon beginning at E9.5 and their neuronal progeny (cre.jax.org). Therefore, to assess brain size we generated *Emx1-Cre;* $Magoh^{lox/+}$ mice and collected postnatal day 12 (P12) brains. Compared to *Emx1-Cre*/+ controls, *Emx1-Cre;* $Magoh^{lox/+}$ brains were significantly smaller (n=3, each genotype) ($P<0.001$) (Figs. 3a,b). Smaller brain size was also evident in E16.5 $Magoh^{del/+}$ brain sections (Fig. 3c). In contrast, no microcephalic phenotype was observed in $Magoh^{lox/lox}$ brains without Cre (data not shown).

To compare the germline and conditional phenotypes we quantified cortical thickness of $Magoh^{del/+}$, $Magoh^{Mos2/+}$, and *Emx1-Cre;* $Magoh^{lox/+}$ E16.5 brains (Figs. 3d,e). As previously observed, $Magoh^{Mos2/+}$ cortical thickness was approximately 50% that of the control ($P<0.001$) (Silver et al. 2010). $Magoh^{del/+}$ cortical thickness was also significantly reduced, although to a slightly lesser extent than $Magoh^{Mos2/+}$. We attribute this small phenotypic difference to the distinct genetic backgrounds of $Magoh^{del/+}$ and $Magoh^{Mos2/+}$, which are on FVB/B6 and B6, respectively. *Emx1-Cre;* $Magoh^{lox/+}$ brains were also significantly thinner than control, but thicker than $Magoh^{Mos2/+}$. The thicker cortex of *Emx1-Cre;* $Magoh^{lox/+}$ brains is likely due to a contribution of ventrally derived neurons, which migrate into the dorsal telencephalon, but are not targeted by *Emx1-Cre* (Greig et al. 2013). Together these data indicate that conditional deletion of *Magoh* during embryonic brain development causes microcephaly, as previously reported for $Magoh^{Mos2/+}$ mice (Silver et al. 2010).

Magoh$^{Mos2/+}$ haploinsufficient mice also exhibit hypopigmentation in adults, due to defective neural crest-derived melanoblast development (Silver et al. 2013). Thus we assessed pigmentation in adult *Magoh*$^{del/+}$ mice. *Magoh*$^{del/+}$ mice were viable, in contrast to inbred C57BL/6J *Magoh*$^{Mos2/+}$ mice which die perinatally (Silver et al. 2010). We attribute this difference to the mixed genetic background of *Magoh*$^{del/+}$ mice leading to hybrid vigor, as *Ddx4- Cre* is on an FVB background while the *Magoh*$^{lox/lox}$ mice were generated on a C57BL/6J background. Adult *Magoh*$^{del/+}$ mice exhibited white belly spots and dorsal hypopigmentation (Fig. 4), thus recapitulating the pigmentation defect observed in *Magoh*$^{Mos2/+}$ adult mice (Silver et al. 2013). This indicates that ubiquitous conditional deletion of *Magoh* results in hypopigmentation.

In conclusion, our study establishes the *Magoh* conditional allele as a new genetic tool to assess *Magoh* function. Importantly we demonstrate that Cre-mediated deletion of *Magoh* results in a loss-of-function null allele. This is based upon molecular evidence that *Magoh* mRNA and protein levels are reduced by 50% in *Magoh*$^{del/+}$ mice. The nature of this allele is also demonstrated using two different Cre drivers to recapitulate null phenotypes of microcephaly and hypopigmentation, which were previously evidenced in the *Magoh*$^{Mos2/+}$ germline mutant.

We anticipate this mouse will be useful for understanding *Magoh* function in prenatal and postnatal development, as well as in adult homeostasis. *Magoh* is expressed throughout prenatal development in various highly proliferative tissues, including the brain, the lung, the peripheral nervous system, and the germline (Silver et al. 2010; Visel, Thaller, and Eichele 2004). The conditional *Magoh* allele will enable investigators to assess spatial and temporal specific deletion of *Magoh* in these developing tissues. It will also facilitate studies of how *Magoh* homozygous null cells influence development. These studies are particularly important in light of the observation that in humans, EJC mutations impact development of tissues both within and outside of the brain (Albers et al. 2012; Favaro et al. 2014; Tarpey et al. 2007). *Magoh* also continues to be expressed in postnatal tissues, including the dentate gyrus of the adult brain (Singh et al. 2013) (Allen Brain Atlas). The existing *Magoh*$^{Mos2/+}$ allele is perinatal lethal, currently prohibiting postnatal analysis. Thus this new allele will also be useful for understanding roles for *Magoh* in postnatal development and adult homeostasis. Taken together the *Magoh* conditional allele we report here will be instrumental for future studies aimed at understanding *Magoh* functions.

Methods

Mouse husbandry

The following strains were acquired from Jackson labs: Flp Deleter mice (B6 (C3)-Tg(Pgk1-FLPo)10Sykr/J), *Vasa-Cre* mice (FVB-Tg(*Ddx4*-cre)1Dcas/J), and *Emx1-Cre* (B6.129S2-*Emx1*tm1(cre)Krj/J). *Magoh*$^{lox/lox}$ mice were bred onto C56BL/6J strain. This mouse line will be made available to the research community. All experiments were performed in agreement with the guidelines from the Division of Laboratory Animal Resources from Duke University School of Medicine and IACUC.

Generation of conditional *Magoh* allele

A glycerol stock for the targeting vector, PRPGS00072_A_G06, was obtained from the KOMP consortium. Individual clones were selected by PCR screen of colonies from this stock. The targeting vector was electroporated by the Duke University mouse transgenic facility. 14 positive clones were detected out of a total of 194 clones by both southern blot and PCR of both arms. For long-range PCR of 5′ arms, the following conditions were used: 94°C × 2 min (1×); 94°C × 15 sec, 60°C ×15sec, 68°C × 15sec (40×); 72°C × 7 min.

5′F1: TGGGCCATTTTACCTGAAGAGGTGGAAATAG;

5′R1: CTTTCTAGAGAATAGGAACTTCGGAATAGGAAC.

For long-range PCR of 3′ arms, the following conditions were used: 94°C × 3 min (1×); 94°C × 30 sec, 58°C × 30 sec, 72°C × 30 sec (40×); 72°C × 7 min.

3′F1: CATACATTATACGAAGTTATGGTCTGAGCT;

3′R1: TCCTGGACAGTCATAGCTAGATAATAAGAG.

For southern analysis, 5′ and 3′ probes (approximately 930 bp each) were generated from PCR fragments using the following primers:

5′ arm PCR forward primers: (5F) GAAACCCAGATGCAGTTCTCGGAT

5′ arm PCR reverse primers: (FRTR) CTTTCTAGAGAATAGGAACTTCGGAATAGGAAC

3′ arm PCR forward primers: (LOXPFF) CATACATTATACGAAGTTATGGTCTGAGCT

3′ arm PCR reverse primers: (14KR) CATTCCTGACAATAATCCGGCAATAGC

The following conditions were used: 94°C × 1 min (1×); 94°C × 15 sec, 58°C × 15 sec, 72°C × 10 sec (40×); 72°C × 1 min. Following PCR, the product was treated with DpnI for 2 hours and purified. The DNA probes were labeled using Alkaline Phosphatase labeling (Amersham AlkPhos Direct labeling Reagents, GE). Genomic DNA was digested overnight using either PvuII (for 5′ arm) or EcoRV (for 3′ arm) and 3 μg of DNA was loaded onto agarose gels. Gel transfer was performed using standard methods including using a UV stratalinker. Blots were hybridized and washed at 60 °C, and developed after 6 days, according to manufacturer protocol (Amersham AlkPhos Direct labeling Reagents, GE).

Genotyping

For genotyping $Magoh^{lox}$ mice: the following primers were used:

LoxF1: AAAGCATCTACAGGAGTAGCAAGTGTCATA

LoxR1: AGGTCTGTACCTCTTTCCTGATCATGACGT.

For genotyping $Magoh^{del/+}$ mice:

LoxF1: AAAGCATCTACAGGAGTAGCAAGTGTCATA

LoxR2: GATGGGTTTCCACAGTAAAAGGAGGCAAAATG

For both genotyping assays the following conditions were used: 94°C × 3 min (1×); 94°C × 30 sec, 58°C × 30 sec, 72°C × 40 sec (35×); 72°C × 7 min.

Western blot and qRT-PCR analysis

E12.5 embryonic cortices were collected from control and *Magoh*$^{del/+}$ mice and lysed in RIPA lysis buffer with protease inhibitors (Pierce, Rockford, IL). Cortical lysates were run on 4–12% SDS-Polyacrylamide gels (Bio-Rad). Gels were transferred onto nitrocellulose membranes and blotted using the following primary antibodies: rabbit anti-Magoh (1:400, Proteintech), mouse anti-α-Tubulin (1:1,000, Sigma). Blots were developed using ECL reagent (Pierce). Densitometry was performed using ImageJ. Final values were quantified by normalizing Magoh levels to loading controls (α-Tubulin). E12.5 embryonic cortices were collected from 3-4 control and *Magoh*$^{del/+}$ embryos and RNA was extracted using the RNeasy kit (Qiagen). cDNA was prepared according to the iScript kit (Bio-Rad). qPCR was performed in triplicates using Taqman probes (Life Technologies): *Magoh* (Mm00487546_m1), *GAPDH* (4352339E). Values were normalized to *GAPDH* control.

Histology and Brain Size Quantifications

Brains were fixed overnight in 4% PFA, followed by submersion in 30% sucrose until sinking, as previously described (Silver et al. 2010). 20μm brain cryostat sections were prepared and incubated with hoechst for 15 min at room temp. High magnification images were captured using a Zeiss apotome. Quantifications of cortical thickness were performed using Zen software (Zeiss). Three sections from anatomically comparable regions were quantified per embryo. Cortical thickness was measured at three points in the dorsal telencephalon per section. Average thickness per biological replicate was then used for statistical analysis (ANOVA). Whole-mount brain area was measured in ImageJ, by outlining an entire hemisphere of the cortex and measuring the relative area (students' t-test).

Supplementary Material

Refer to Web version on PubMed Central for supplementary material.

Acknowledgments

The authors acknowledge funding from NINDS/NIH, R01NS083897 (to D.L.S.) and 5T32NS051156-09 (to J.J.M.). Additionally the authors thank the Duke Transgenic mouse facility for assistance in generation of the *Magoh*$^{lox/lox}$ conditional mouse. Finally the authors thank members of the Silver laboratory for helpful discussions.

References

Addington AM, Gauthier J, Piton A, Hamdan FF, Raymond A, Gogtay N, Miller R, et al. A Novel Frameshift Mutation in UPF3B Identified in Brothers Affected with Childhood Onset Schizophrenia and Autism Spectrum Disorders. Molecular Psychiatry. 2011; 16(3):238–39.10.1038/mp.2010.59 [PubMed: 20479756]

Albers, Cornelis A.; Paul, Dirk S.; Schulze, Harald; Freson, Kathleen; Stephens, Jonathan C.; Smethurst, Peter A.; Jolley, Jennifer D., et al. Compound Inheritance of a Low-Frequency Regulatory SNP and a Rare Null Mutation in Exon-Junction Complex Subunit RBM8A Causes TAR Syndrome. Nature Genetics. 201210.1038/ng.1083

Ashton-Beaucage, Dariel; Udell, Christian M.; Lavoie, Hugo; Baril, Caroline; Lefrançois, Martin; Chagnon, Pierre; Gendron, Patrick, et al. The Exon Junction Complex Controls the Splicing of MAPK and Other Long Intron-Containing Transcripts in Drosophila. Cell. 2010; 143(2):251–62.10.1016/j.cell.2010.09.014 [PubMed: 20946983]

Bono, Fulvia; Gehring, Niels H. Assembly, Disassembly and Recycling: the Dynamics of Exon Junction Complexes. RNA Biology. 2011; 8(1):24–29. [PubMed: 21289489]

Favaro, Francine P.; Alvizi, Lucas; Zechi-Ceide, Roseli M.; Bertola, Debora; Felix, Temis M.; de Souza, Josiane; Raskin, Salmo, et al. A Noncoding Expansion in EIF4A3 Causes Richieri-Costa-Pereira Syndrome, a Craniofacial Disorder Associated with Limb Defects. American Journal of Human Genetics. 2014; 94(1):120–28.10.1016/j.ajhg.2013.11.020 [PubMed: 24360810]

Greig, Luciano Custo; Woodworth, Mollie B.; Galazo, Maria J.; Padmanabhan, Hari; Macklis, Jeffrey D. Nature Publishing Group. Vol. 14. Nature Publishing Group; 2013. Molecular Logic of Neocortical Projection Neuron Specification, Development and Diversity; p. 755-69.

Kataoka N, Diem MD, Kim VN, Yong J, Dreyfuss G. Magoh, a Human Homolog of Drosophila Mago Nashi Protein, Is a Component of the Splicing-Dependent Exon-Exon Junction Complex. The EMBO Journal. 2001; 20(22):6424–33.10.1093/emboj/20.22.6424 [PubMed: 11707413]

Le Hir H, Gatfield D, Braun IC, Forler D, Izaurralde E. The Protein Mago Provides a Link Between Splicing and mRNA Localization. EMBO Reports. 2001; 2(12):1119–24.10.1093/embo-reports/kve245 [PubMed: 11743026]

Matera, Ivana; Watkins-Chow, Dawn E.; Loftus, Stacie K.; Hou, Ling; Incao, Arturo; Silver, Debra L.; Rivas, Cecelia; Elliott, Eugene C.; Baxter, Laura L.; Pavan, William J. A Sensitized Mutagenesis Screen Identifies Gli3 as a Modifier of Sox10 Neurocristopathy. Human Molecular Genetics. 2008; 17(14):2118–31.10.1093/hmg/ddn110 [PubMed: 18397875]

Nguyen LS, Kim HG, Rosenfeld JA, Shen Y, Gusella JF, Lacassie Y, Layman LC, Shaffer LG, Gécz J. Contribution of Copy Number Variants Involving Nonsense-Mediated mRNA Decay Pathway Genes to Neuro-Developmental Disorders. Human Molecular Genetics. 2013; 22(9):1816–25.10.1093/hmg/ddt035 [PubMed: 23376982]

Nott, Ajit; Le Hir, Hervé; Moore, Melissa J. Splicing Enhances Translation in Mammalian Cells: an Additional Function of the Exon Junction Complex. Genes & Development. 2004; 18(2):210–22.10.1101/gad.1163204 [PubMed: 14752011]

Palacios, Isabel M.; Gatfield, David; St Johnston, Daniel; Izaurralde, Elisa. An eIF4AIII-Containing Complex Required for mRNA Localization and Nonsense-Mediated mRNA Decay. Nature. 2004; 427(6976):753–57.10.1038/nature02351 [PubMed: 14973490]

Roignant, Jean-Yves; Treisman, Jessica E. Exon Junction Complex Subunits Are Required to Splice Drosophila MAP Kinase, a Large Heterochromatic Gene. Cell. 2010; 143(2):238–50.10.1016/j.cell.2010.09.036 [PubMed: 20946982]

Sharp, Andrew J.; Hansen, Sierra; Selzer, Rebecca R.; Cheng, Ze; Regan, Regina; Hurst, Jane A.; Stewart, Helen, et al. Discovery of Previously Unidentified Genomic Disorders From the Duplication Architecture of the Human Genome. Nature Genetics. 2006; 38(9):1038–42.10.1038/ng1862 [PubMed: 16906162]

Silver, Debra L.; Watkins-Chow, Dawn E.; Schreck, Karisa C.; Pierfelice, Tarran J.; Larson, Denise M.; Burnetti, Anthony J.; Liaw, Hung-Jiun, et al. The Exon Junction Complex Component Magoh Controls Brain Size by Regulating Neural Stem Cell Division. Nature Neuroscience. 2010; 13(5):551–58.10.1038/nn.2527

Silver, Debra L.; Leeds, Karen E.; Hwang, Hun-Way; Miller, Emily E.; Pavan, William J. Developmental Biology. Vol. 375. Elsevier; 2013. The EJC Component Magoh Regulates Proliferation and Expansion of Neural Crest- Derived Melanocytes; p. 172-81.

Singh, Kusum K.; Wachsmuth, Laurens; Kulozik, Andreas E.; Gehring, Niels H. Two Mammalian MAGOH Genes Contribute to Exon Junction Complex Composition and Nonsense-Mediated Decay. RNA Biology. 2013; 10(8):1291–98.10.4161/rna.25827 [PubMed: 23917022]

Tarpey, Patrick S.; Raymond, F Lucy; Nguyen, LS.; Rodriguez, Jayson; Hackett, Anna; Vandeleur, Lucianne; Smith, Raffaella, et al. Mutations in UPF3B, a Member of the Nonsense-Mediated mRNA Decay Complex, Cause Syndromic and Nonsyndromic Mental Retardation. Vol. 39. Nature Publishing Group; 2007. p. 1127-33.

Visel, Axel; Thaller, Christina; Eichele, Gregor. GenePaint.org: an Atlas of Gene Expression Patterns in the Mouse Embryo. Nucleic Acids Research. 2004; 32(Database issue):D552–56.10.1093/nar/gkh029 [PubMed: 14681479]

Zhao XF, Nowak NJ, Shows TB, Aplan PD. MAGOH Interacts with a Novel RNA-Binding Protein. Genomics. 2000; 63(1):145–48.10.1006/geno.1999.6064 [PubMed: 10662555]

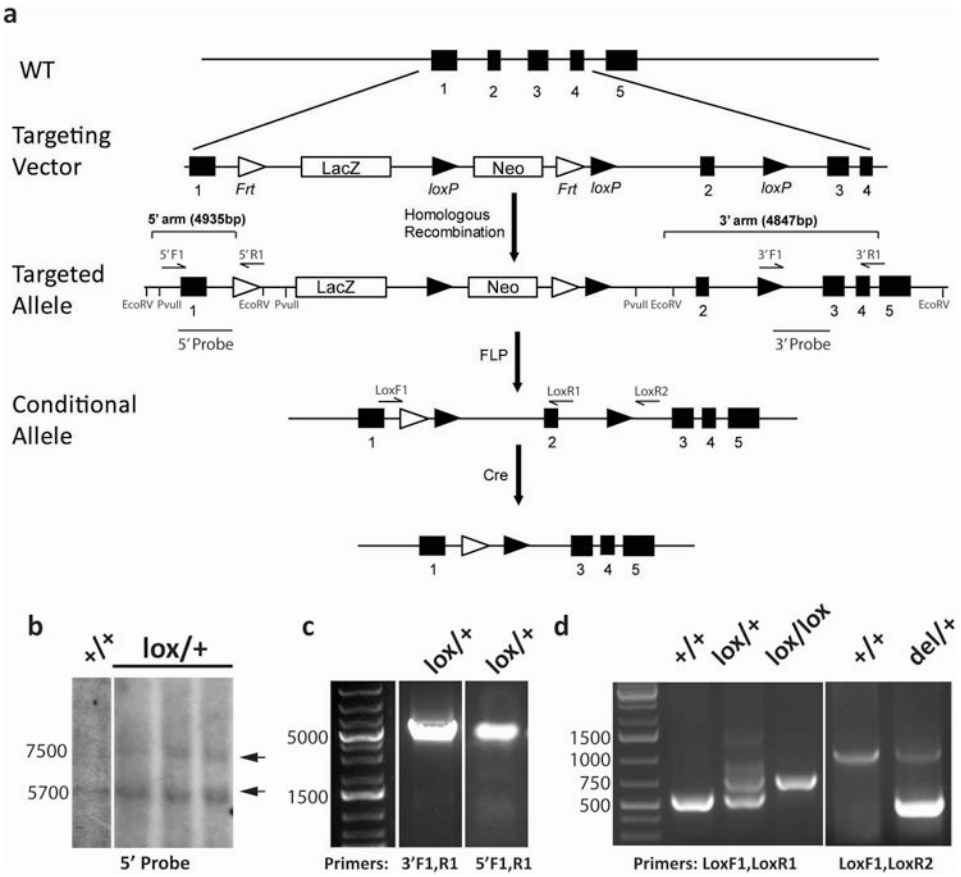

Figure 1. Generation Of A *Magoh* Conditional Allele

(a) Schematic of wild-type genomic locus of *Magoh* with 5 exons (black boxes) and introns (lines, not to scale). Targeting scheme showing targeting vector and targeted allele with 2 *loxP* sites (black arrowheads) flanking exon 2, neo and LacZ cassettes, and 2 FRT sites. Primers for long-range PCR of ES cells and genotyping are shown as arrows, southern blot probes are indicated as black lines, and restriction enzyme sites are noted. The conditional alleles following *Flp* recombination or following *Cre* recombination are shown. (b) Representative southern blot analysis of *PvuI1* digested genomic DNA showing screen of the 5′ arm in ES cells. Note a single band at 5.7 Kb is observed in control, while two bands at 5.7 Kb and 7.3 Kb are detected in *lox*/+ samples. (c) Representative long-range PCR results for screening of the 3′ arm and 5′ arm in ES cells. (d) (left panel) Representative PCR genotyping results from control (+/+), heterozygous (*lox*/+), and homozygous (*lox/lox*) mice. Note a 561 bp band in +/+, 561 bp and 678 bp bands in *lox*/+, and a 678 bp band in *lox/lox*. (right panel) PCR genotyping results from +/+ and $Magoh^{del/+}$ mice. Note a 1250 bp band in +/+ and both 1250 bp and 420 bp bands in $Magoh^{del/+}$.

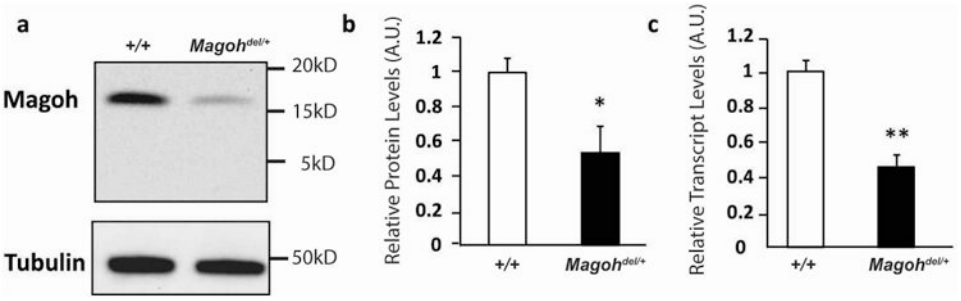

Figure 2. *Magoh* mRNA and protein levels are reduced in *Magoh*$^{del/+}$ conditional mice

(a) Representative western blot depicting +/+ and *Magoh*$^{del/+}$ E12.5 cortical brain lysates probed for anti-Magoh or anti-α-Tubulin. Note a single 17KDa band is evident in *Magoh*$^{del/+}$ brains at reduced levels compared to +/+. (b) Quantification of Magoh protein levels by densitometry of western blots, following normalization for loading. (c) Quantification of *Magoh* mRNA levels in E12.5 +/+ and *Magoh*$^{del/+}$ cortices, following normalization using *Gapdh*. n= 3-4 for all samples, *, $P<0.05$, **, $P<0.01$.

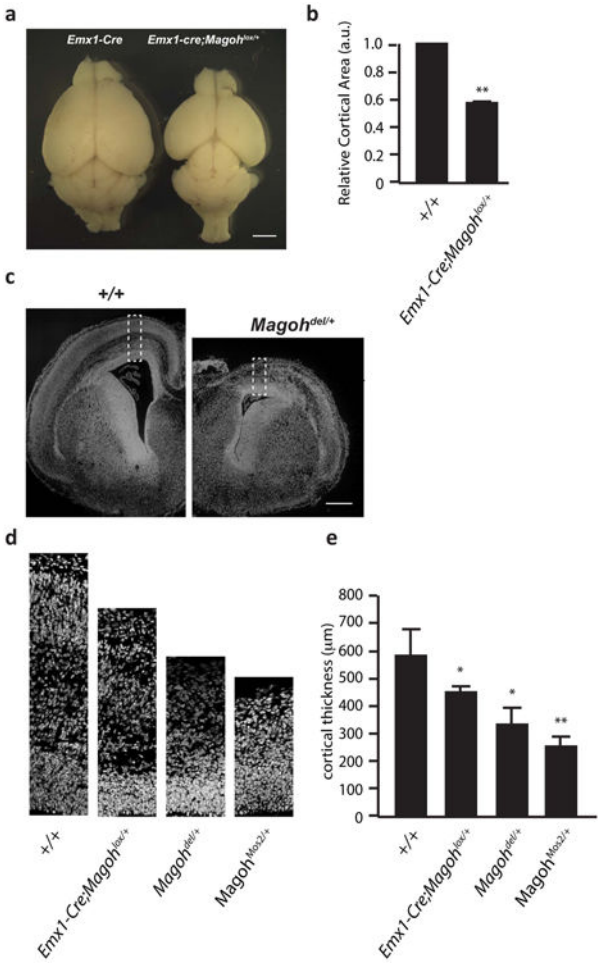

Figure 3. Ubiquitous or brain specific conditional deletion of *Magoh* causes microcephaly

(a) Images of whole mount brains collected at postnatal day 12 from *Emx1-Cre* and *Emx1-Cre; Magoh*$^{lox/+}$ mice (scale bar = 2mm). (b) Quantification of relative cortical area in P12 *Emx1-Cre* and *Emx1-Cre; Magoh*$^{lox/+}$ mice. (c) Coronal sections from E16.5 control (+/+) and *Magoh*$^{del/+}$ brains stained for nuclei (DAPI, white) (scale bar = 200μm). (d) Higher magnification representative images of coronal sections in +/+, *Emx1-Cre; Magoh*$^{lox/+}$, *Magoh*$^{del/+}$, and *Magoh*$^{Mos2/+}$. (e) Quantification of cortical thickness in +/+, *Emx1-Cre; Magoh*$^{lox/+}$, *Magoh*$^{del/+}$, and *Magoh*$^{Mos2/+}$ mice. *, $P<0.05$, **, $P<0.01$; n=3-4 biological replicates.

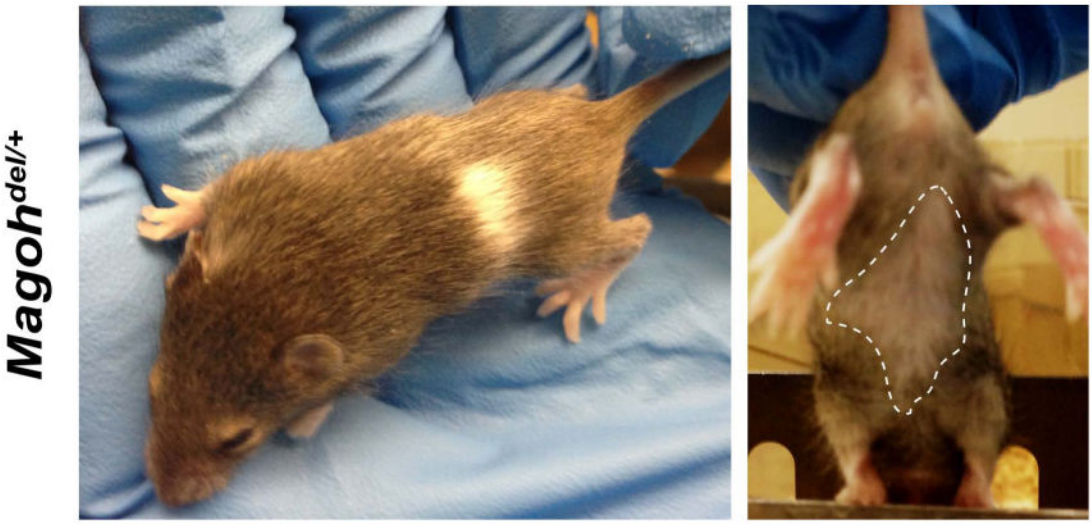

Figure 4. Ubiquitous conditional depletion of *Magoh* causes hypopigmentation

Two different views of adult *Magoh*$^{del/+}$ mice reveal dorsal hypopigmentation (left panel) and ventral hypopigmentation (right panel). A dotted line demarcates the ventral hypopigmented spot on the right.